Dalton Transactions

Gd^{3+}-activated narrowband ultraviolet-B persistent luminescence through persistent energy transfer

Journal:	*Dalton Transactions*
Manuscript ID	DT-ART-01-2021-000120.R1
Article Type:	Paper
Date Submitted by the Author:	15-Feb-2021
Complete List of Authors:	Wang, Xianli; University of Georgia, College of Engineering Chen, Yafei; King Fahd University of Petroleum & Minerals Kner, Peter ; University of Georgia , College of Engineering Pan, Zhengwei; King Fahd University of Petroleum & Minerals, Center for Integrative Petroleum Research

ARTICLE

Gd^{3+}-activated narrowband ultraviolet-B persistent luminescence through persistent energy transfer†

Received 00th January 2021,
Accepted 00th January 2021

DOI: 10.1039/x0xx00000x

Xianli Wang,[a‡] Yafei Chen,[b‡] Peter A. Kner[a] and Zhengwei Pan*[b]

This work reports the realization of Gd^{3+} persistent luminescence in the narrowband ultraviolet-B (NB-UVB; 310–313 nm) through persistent energy transfer from a sensitizer of Pr^{3+}, Pb^{2+} or Bi^{3+}. We propose a general design concept to develop Gd^{3+}-activated NB-UVB persistent phosphors from Pr^{3+}-, Pb^{2+}- or Bi^{3+}-activated ultraviolet-C (200–280 nm) or ultraviolet-B (280–315 nm) persistent phosphors, leading to the discovery of ten Gd^{3+} NB-UVB persistent phosphors such as $Sr_3Gd_2Si_6O_{18}:Pr^{3+}$, $Sr_3Gd_2Si_6O_{18}:Pb^{2+}$ and $Y_2GdAl_2Ga_3O_{12}:Bi^{3+}$ as well as five ultraviolet-B persistent phosphors such as $Y_3Al_2Ga_3O_{12}:Pr^{3+}$, $Sr_3Y_2Si_6O_{18}:Pb^{2+}$ and $Y_3Al_2Ga_3O_{12}:Bi^{3+}$. The persistent energy transfer from the sensitizers to Gd^{3+} is very efficient and the Gd^{3+} NB-UVB afterglow can last for more than 10 hours. This study expands the persistent luminescence research to the NB-UVB as well as the broader ultraviolet-B spectral regions. The NB-UVB persistent phosphors may act as self-sustained glowing NB-UVB radiation sources for dermatological therapy.

Introduction

Ultraviolet-B (UVB) spectral band refers to the spectrum of light in the range of 280–315 nm. UVB light in the natural solar spectrum has been used for centuries in the treatment of various skin disorders such as psoriasis and vitiligo.[1,2] Action spectrum studies of UVB wavelengths for psoriasis carried out in the late 1970s revealed that it is the narrowband UVB (NB-UVB; 310–313 nm) emission that is most effective for phototherapy.[3–5] These findings quickly led to the development and use of artificial NB-UVB light sources for dermatological therapy.[6–10] Currently, phototherapy based on Philips TL-01 NB-UVB fluorescent tubes is the treatment of choice for various skin disorders which affect millions of people around the world.[11,12]

In developing phosphors for NB-UVB fluorescent tubes, Gd^{3+} is consistently used as the emitter,[13–17] because the Gd^{3+} $^6P_{7/2} \rightarrow {}^8S_{7/2}$ emission transition gives efficient line emission at 311 nm, which is within the action spectrum of phototherapy. However, due to the forbidden nature of the transitions within the Gd^{3+} $4f^7$ configuration, Gd^{3+} has very poor optical absorption of 200–300 nm excitation light. To make the Gd^{3+}-activated phosphors "excitable" by the short-wavelength UV light, a sensitizer is needed. The role of the sensitizer is to absorb the excitation energy and to transfer it to Gd^{3+}. Accordingly, the emitting levels of the sensitizer should be resonant with the excited states (*i.e.*, ^6I_J or ^6P_J states) of Gd^{3+}. The available sensitizers for Gd^{3+} photoluminescence include Pr^{3+} (*e.g.*, $Y_2GdAl_5O_{12}:Pr^{3+}$, $GdBO_3:Pr^{3+}$, $LaPO_4:Pr^{3+},Gd^{3+}$),[13–16] Pb^{2+} (*e.g.*, $GdBO_3:Pb^{2+}$),[17] Bi^{3+} (*e.g.*, $LaB_3O_6:Bi^{3+},Gd^{3+}$; the phosphor used in the Philips TL-01 fluorescent tubes),[6] and Ce^{3+} (*e.g.*, $GdMgB_5O_{10}:Ce^{3+}$).[18] Among these sensitizers, the ^6I_J or ^6P_J excited states of Gd^{3+} overlap with the 4f5d emitting level of Pr^{3+}, the $^3P_1$ emitting level of Pb^{2+}, the $^3P_1$ emitting level of Bi^{3+}, or the 5d emitting level of Ce^{3+}.

The Gd^{3+}-activated NB-UVB phosphors developed by far are photoluminescent, where continuous external excitation is needed. Here, we report the design and fabrication of a new type of Gd^{3+}-activated NB-UVB phosphors, *i.e.*, Gd^{3+}-activated NB-UVB persistent phosphors, which can emit Gd^{3+} 311 nm persistent luminescence (also called afterglow) without the need of constant external excitation. For a persistent phosphor to work, the host should contain appropriate energy traps that can capture and store the excitation energy (in the form of electrons through the excitation of the activator) during the excitation and, after the excitation is ceased, gradually release the trapped electrons to the activator to produce persistent luminescence.[19,20] For Gd^{3+}, however, since it has a stabilized $4f^7$ configuration, it has no tendency to be oxidized or reduced in a phosphor. Consequently, there is no electron transfer between Gd^{3+} and the trapping states, and therefore Gd^{3+} cannot directly play the role of persistent luminescence emitting center in a persistent phosphor.[21] Since Pr^{3+}, Pb^{2+}, Bi^{3+} and Ce^{3+} are efficient steady-state sensitizers for Gd^{3+} photoluminescence in some hosts,[6,13–18] we propose to expand their use as persistent sensitizers to persistently transfer energy to Gd^{3+} to produce Gd^{3+} NB-UVB persistent luminescence (note that persistent energy transfer strategy was previously used to design and fabricate visible- and infrared-emitting persistent phosphors).[22–24] Taking Pr^{3+} as the persistent sensitizer, this persistent energy transfer process can be illustrated by the schematic Pr^{3+}–Gd^{3+} energy transfer diagram in Fig.

[a] College of Engineering, University of Georgia, Athens, GA 30602, USA.
[b] Centre for Integrative Petroleum Research, College of Petroleum Engineering and Geosciences, King Fahd University of Petroleum & Minerals, Dhahran 31261, KSA.
‡ These authors contributed equally to this work.
* E-mail: zhengwei.pan@gmail.com

† Electronic Supplementary Information (ESI) available: XRD patterns of NB-UVB persistent phosphors $Sr_3Gd_2Si_6O_{18}:Pr^{3+}$, $Sr_3Gd_2Si_6O_{18}:Pb^{2+}$, $Y_2GdAl_2Ga_3O_{12}:Pr^{3+}$ and $Y_2GdAl_2Ga_3O_{12}:Bi^{3+}$, persistent luminescence properties of NB-UVB persistent phosphors $Ca_{1.8}Gd_{0.2}Al_2SiO_7:Pr^{3+}$, $Lu_{1.8}Gd_{0.2}SiO_5:Pr^{3+}$, $Ca_{2.8}Gd_{0.2}Al_2Si_3O_{12}:Pr^{3+}$, $LiY_{0.8}Gd_{0.2}SiO_4:Pr^{3+}$, $Sr_3Y_{2-x}Gd_xSi_6O_{18}:Pb^{2+}$, $Lu_2GdAl_2Ga_3O_{12}:Pr^{3+}$ and $Lu_2GdAl_2Ga_3O_{12}:Bi^{3+}$, persistent luminescence properties of UVB persistent phosphors $Lu_3Al_2Ga_3O_{12}:Pr^{3+}$ and $Lu_3Al_2Ga_3O_{12}:Bi^{3+}$, and conceptual self-sustained NB-UVB Band-Aid phototherapy.

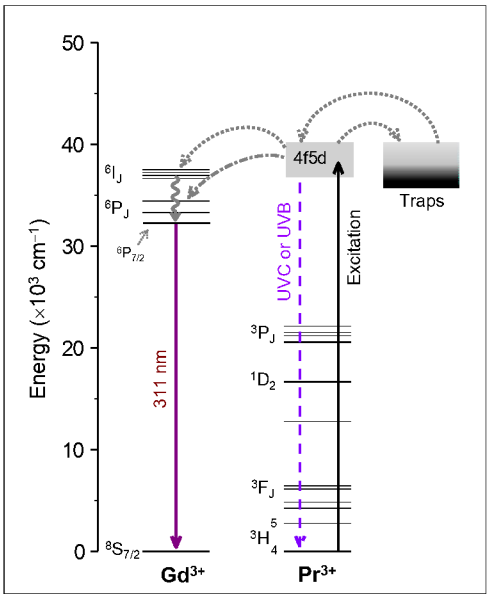

Fig. 1 Schematic representation of persistent energy transfer from Pr^{3+} to Gd^{3+} in a NB-UVB persistent phosphor. Under high-energy UV light (*e.g.*, 254 nm light) excitation, Pr^{3+} ions absorb the excitation energy which is then stored (in the form of electrons) in the energy traps in the material. After the excitation is ceased, the captured energy is thermally released to the Pr^{3+} 4f5d emitting level, which is then persistently transferred to the Gd^{3+} ^6I_J levels or ^6P_J levels, subsequently producing persistent emission at 311 nm via the Gd^{3+} $^6P_{7/2} \rightarrow {}^8S_{7/2}$ emission transition. Straight-line arrows and curved-line arrows represent optical transitions and electron transfer processes, respectively.

1. Besides the sensitizer function, Pr^{3+} should also function as a persistent luminescence activator. However, instead of giving out its own persistent emission in the ultraviolet-C (UVC; 200–280 nm) or the UVB via the Pr^{3+} 4f5d $\rightarrow {}^3H_{4,5}$ emission transitions, the energy released to the Pr^{3+} 4f5d emitting state from the trapping states is continuously and efficiently transferred to the Gd^{3+} ^6I_J levels (~35,700–37,000 cm^{-1}, corresponding to ~280–270 nm) or the lower-energy ^6P_J levels (~31,700–33,200 cm^{-1}, corresponding to ~315–301 nm), subsequently producing Gd^{3+} persistent luminescence at 311 nm via the Gd^{3+} $^6P_{7/2} \rightarrow {}^8S_{7/2}$ emission transition. Therefore, we propose that a Gd^{3+}-activated, Pr^{3+}-sensitized NB-UVB persistent phosphor can be designed upon a Pr^{3+}-activated UVC persistent phosphor or a Pr^{3+}-activated UVB persistent phosphor. This design principle is also valid for other sensitizers of Gd^{3+}.

Recently, we developed five types of Pr^{3+}-activated, silicate-based UVC persistent phosphors that emit long-time persistent luminescence peaking at 265–270 nm.[25] These Pr^{3+}-activated UVC persistent phosphors provide us an ideal platform to test the Pr^{3+} to Gd^{3+} persistent energy transfer and our concept of designing Gd^{3+}-activated NB-UVB persistent phosphors. Here we use one type of UVC persistent phosphor, the cyclosilicate structured $Sr_3Y_2Si_6O_{18}:Pr^{3+}$, as the benchmark material to demonstrate the design of a Gd^{3+}-activated, Pr^{3+}-sensitized NB-UVB persistent phosphor, *i.e.*, $Sr_3Gd_2Si_6O_{18}:Pr^{3+}$. To further demonstrate the universality of the design concept, we also specially developed five first-ever Pr^{3+}-, Pb^{2+}- and Bi^{3+}-activated UVB persistent phosphors, represented by $Y_3Al_2Ga_3O_{12}:Pr^{3+}$, $Sr_3Y_2Si_6O_{18}:Pb^{2+}$ and $Y_3Al_2Ga_3O_{12}:Bi^{3+}$, respectively, and used them to fabricate Gd^{3+} NB-UVB persistent phosphors $Y_2GdAl_2Ga_3O_{12}:Pr^{3+}$, $Sr_3Gd_2Si_6O_{18}:Pb^{2+}$ and $Y_2GdAl_2Ga_3O_{12}:Bi^{3+}$. In these NB-UVB persistent phosphors, the persistent energy transfer from the sensitizers to Gd^{3+} is very efficient and the Gd^{3+} NB-UVB afterglow can last for more than 10 h.

Experimental

Materials synthesis

All the phosphors discussed in this work were fabricated using a solid-state reaction method. Taking the synthesis of $Sr_3Gd_2Si_6O_{18}:Pr^{3+}$ phosphor as an example, stoichiometric amounts of $SrCO_3$, Gd_2O_3, SiO_2 and Pr_6O_{11} powders (Pr^{3+} content, 1 atom%) were ground to form a homogeneous fine powder. The mixed powder was prefired at 900 °C in air for 2 h. The prefired powder was ground again and was then pressed into 15-mm-diameter discs using a hydraulic press. The disc samples were then sintered at 1250 °C in air for 2 h to form solid ceramic discs.

Characterization of crystal structures

The X-ray diffraction patterns (XRD) of some phosphors were recorded using a PANalytical X'Pert PRO powder X-ray diffractometer with Cu Kα1 radiation (λ = 1.5406 Å).

Spectroscopic measurements

The steady-state photoluminescence properties of the phosphors were recorded using a McPherson spectrometer, which comprises of a McPherson Model 234/302 excitation monochromator and a McPherson Model 2035 emission monochromator. The persistent luminescence properties were measured using a Horiba FluoroLog-3 spectrofluorometer equipped with a R928P photomultiplier tube. An Ocean Optics QEPRO spectrometer was also used to record the persistent luminescence emission spectra. In decay-related measurements, a 254 nm mercury lamp was used to charge the samples.

Results and discussion

We firstly discuss the $Sr_3Gd_2Si_6O_{18}:Pr^{3+}$ NB-UVB persistent phosphor developed from the $Sr_3Y_2Si_6O_{18}:Pr^{3+}$ UVC persistent phosphor. The as-synthesized $Sr_3Gd_2Si_6O_{18}:Pr^{3+}$ compound has the cyclosilicate structure, which shares the same structure as the benchmark compound $Sr_3Y_2Si_6O_{18}$ (ICDD 00-065-0204)[26] (Fig. S1a, ESI†). In the $Sr_3Gd_2Si_6O_{18}:Pr^{3+}$ phosphor, Pr^{3+} ions occupy the Sr/Gd sites with eightfold coordination.[25] Figure 2a shows the normalized photoluminescence excitation and emission spectra of $Sr_3Gd_2Si_6O_{18}:Pr^{3+}$, $Sr_3Y_2Si_6O_{18}:Pr^{3+}$ and $Sr_3Gd_2Si_6O_{18}$ phosphors. The spectra of the Gd^{3+}-free $Sr_3Y_2Si_6O_{18}:Pr^{3+}$ phosphor and the Pr^{3+}-free $Sr_3Gd_2Si_6O_{18}$ phosphor are presented to emphasize the sensitizer role of Pr^{3+} in the $Sr_3Gd_2Si_6O_{18}:Pr^{3+}$ phosphor. Under excitation at 249 nm, the $Sr_3Y_2Si_6O_{18}:Pr^{3+}$ phosphor exhibits a strong emission band peaking at ~266 nm and a weak shoulder band peaking at ~308 nm (the blue dash line curve), which can be attributed to the Pr^{3+} 4f5d

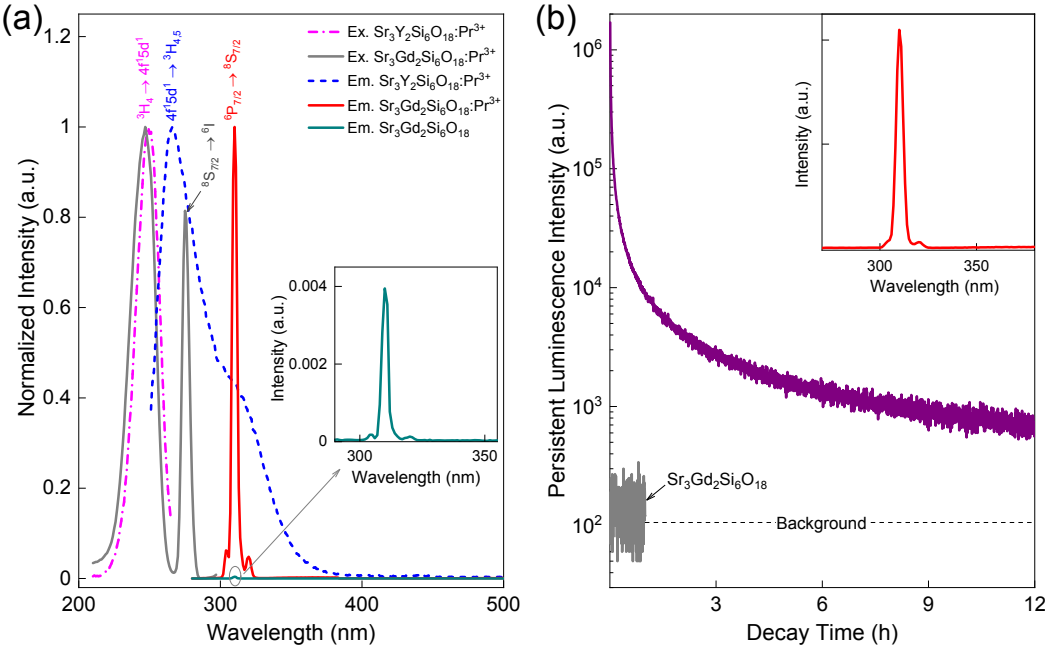

Fig. 2 $Sr_3Gd_2Si_6O_{18}:Pr^{3+}$ NB-UVB persistent phosphor developed from $Sr_3Y_2Si_6O_{18}:Pr^{3+}$ UVC persistent phosphor. (a) Normalized photoluminescence excitation and emission spectra of $Sr_3Gd_2Si_6O_{18}:Pr^{3+}$ NB-UVB persistent phosphor, $Sr_3Y_2Si_6O_{18}:Pr^{3+}$ UVC persistent phosphor and Pr^{3+}-free $Sr_3Gd_2Si_6O_{18}$ host at room temperature. The emission spectra are acquired under 249 nm light excitation and the excitation spectra are obtained by monitoring the 266 nm emission for the $Sr_3Y_2Si_6O_{18}:Pr^{3+}$ phosphor and the 311 nm emission for the $Sr_3Gd_2Si_6O_{18}:Pr^{3+}$ phosphor. The inset is the enlargement of the Gd^{3+} photoluminescence in $Sr_3Gd_2Si_6O_{18}$ host. (b) Persistent luminescence decay curves of $Sr_3Gd_2Si_6O_{18}:Pr^{3+}$ phosphor and $Sr_3Gd_2Si_6O_{18}$ host monitored at 311 nm after irradiation by a 254 nm lamp for 5 min. The inset shows the persistent luminescence emission spectrum of $Sr_3Gd_2Si_6O_{18}:Pr^{3+}$ phosphor recorded at 10 min decay.

$\rightarrow {}^3H_{4,5}$ and 4f5d $\rightarrow {}^4H_6, {}^3F_2$ emission transitions, respectively. No apparent Pr^{3+} $4f^2 \rightarrow 4f^2$ intraconfigurational emission transitions in the visible region are observed. The excitation spectrum monitored at 266 nm emission has a strong broad band peaking at ~249 nm (the magenta dot-dash line curve), which is originated from the Pr^{3+} $^3H_4 \rightarrow$ 4f5d excitation transition. The spectral results show that the $Sr_3Y_2Si_6O_{18}:Pr^{3+}$ phosphor is a good UVC photoluminescent material.

When the Y^{3+} ions in the $Sr_3Y_2Si_6O_{18}:Pr^{3+}$ phosphor are substituted by Gd^{3+} ions, the resulting $Sr_3Gd_2Si_6O_{18}:Pr^{3+}$ material becomes a pure NB-UVB phosphor. Under excitation at 249 nm, the material exhibits a strong, narrow emission band at 311 nm originating from the Gd^{3+} $^6P_{7/2} \rightarrow {}^8S_{7/2}$ emission transition (the red solid line curve). No Pr^{3+} 4f5d $\rightarrow {}^3H_{4,5}$ and 4f5d $\rightarrow {}^4H_6, {}^3F_2$ emission transitions appear in the emission spectrum. The excitation spectrum monitored at the Gd^{3+} 311 nm emission consists of two excitation bands: one strong broad band peaking at 247 nm and one small narrow band peaking at 275 nm (the black solid line curve), which can be, respectively, attributed to the Pr^{3+} $^3H_4 \rightarrow$ 4f5d and Gd^{3+} $^8S_{7/2} \rightarrow {}^6I_J$ excitation transitions. The photoluminescence results clearly show the occurrence of highly efficient energy transfer from Pr^{3+} to Gd^{3+} in the $Sr_3Gd_2Si_6O_{18}:Pr^{3+}$ phosphor. This efficient energy transfer is well reflected in the photoluminescence excitation and emission spectra of the two phosphors. For instance, the complete spectral overlap of the Gd^{3+} $^8S_{7/2} \rightarrow {}^6I_J$ excitation band of $Sr_3Gd_2Si_6O_{18}:Pr^{3+}$ and the Pr^{3+} 4f5d $\rightarrow {}^3H_{4,5}$ emission band of $Sr_3Y_2Si_6O_{18}:Pr^{3+}$, the appearance of the Pr^{3+} $^3H_4 \rightarrow$ 4f5d excitation band in the excitation spectrum of $Sr_3Gd_2Si_6O_{18}:Pr^{3+}$ by monitoring the Gd^{3+} emission, the appearance of the Gd^{3+} $^6P_{7/2} \rightarrow {}^8S_{7/2}$ emission transition in the emission spectrum of $Sr_3Gd_2Si_6O_{18}:Pr^{3+}$ by exciting the Pr^{3+} excitation band, as well as the absence of the Pr^{3+} 4f5d $\rightarrow {}^3H_{4,5}$ UVC emission transitions when exciting the Pr^{3+} excitation band in $Sr_3Gd_2Si_6O_{18}:Pr^{3+}$, all suggest the occurrence of efficient energy transfer from the Pr^{3+} 4f5d emitting state to the Gd^{3+} ^6I_J levels in the $Sr_3Gd_2Si_6O_{18}:Pr^{3+}$ phosphor. Moreover, the sensitizer role of Pr^{3+} in the $Sr_3Gd_2Si_6O_{18}:Pr^{3+}$ phosphor is further underlined by the very weak Gd^{3+} photoluminescence in the Pr^{3+}-free $Sr_3Gd_2Si_6O_{18}$ phosphor (inset of Fig. 2a), where the Gd^{3+} photoluminescence emission intensity is about three orders of magnitude lower than that of $Sr_3Gd_2Si_6O_{18}:Pr^{3+}$ phosphor.

In addition to the steady-state Pr^{3+} to Gd^{3+} energy transfer in photoluminescence, efficient persistent energy transfer from Pr^{3+} to Gd^{3+} also occurs after the excitation is ceased, demonstrating that the $Sr_3Gd_2Si_6O_{18}:Pr^{3+}$ phosphor has the NB-UVB persistent luminescence capability. Figure 2b shows the persistent luminescence decay curve of $Sr_3Gd_2Si_6O_{18}:Pr^{3+}$ phosphor monitored at 311 nm after charged by a 254 nm lamp. The data were recorded as a function of the persistent luminescence intensity versus time and the recording lasted for 12 h. The persistent luminescence intensity decreases quickly in the first one hour and slowly afterward. After 12 h decay, the intensity is still over one order of magnitude higher than the background signal. The inset in Fig. 2b shows the persistent luminescence emission spectrum acquired at 10 min decay. Like the photoluminescence emission spectrum in Fig. 2a, only the characteristic Gd^{3+} line emission appears in the persistent

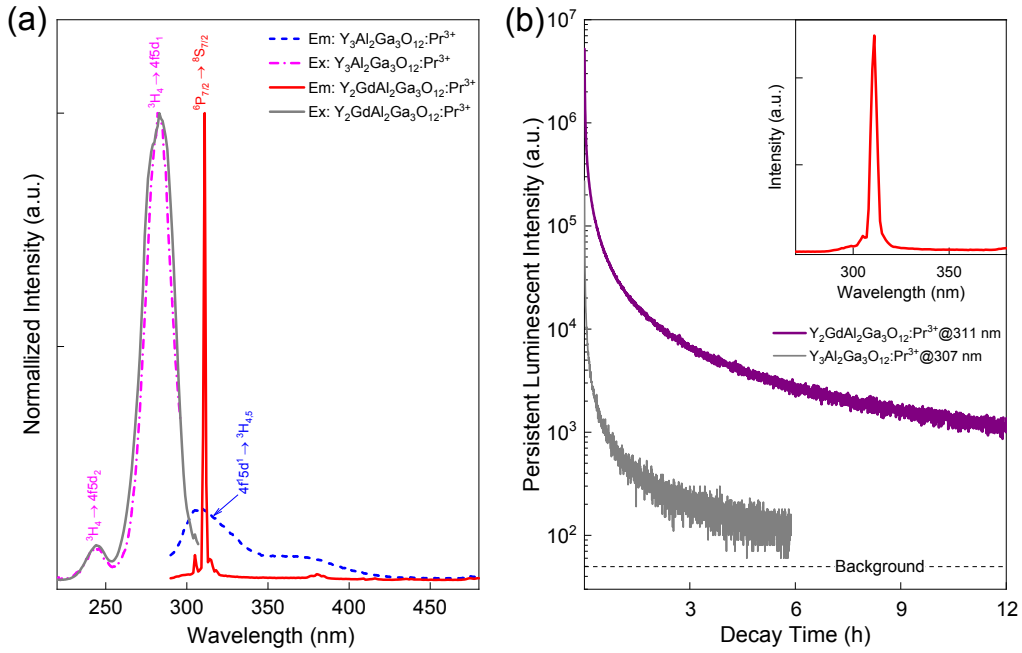

Fig. 3 $Y_2GdAl_2Ga_3O_{12}:Pr^{3+}$ NB-UVB persistent phosphor developed from $Y_3Al_2Ga_3O_{12}:Pr^{3+}$ UVB persistent phosphor. (a) Normalized photoluminescence excitation and emission spectra of $Y_2GdAl_2Ga_3O_{12}:Pr^{3+}$ and $Y_3Al_2Ga_3O_{12}:Pr^{3+}$ phosphors at room temperature. The emission spectra are acquired under 283 nm light excitation and the excitation spectra are obtained by monitoring the 307 nm emission for the $Y_3Al_2Ga_3O_{12}:Pr^{3+}$ phosphor and the 311 nm emission for the $Y_2GdAl_2Ga_3O_{12}:Pr^{3+}$ phosphor. (b) Persistent luminescence decay curves of $Y_3Al_2Ga_3O_{12}:Pr^{3+}$ phosphor monitored at 307 nm and $Y_2GdAl_2Ga_3O_{12}:Pr^{3+}$ phosphor monitored at 311 nm after irradiation by a 254 nm lamp for 5 min. The inset shows the persistent luminescence emission spectrum of $Y_2GdAl_2Ga_3O_{12}:Pr^{3+}$ phosphor recorded at 10 min decay.

luminescence emission spectrum. In stark contrast, no Gd^{3+} persistent luminescence signal is detected in the Pr^{3+}-free $Sr_3Gd_2Si_6O_{18}$ phosphor (Fig. 2b), which strongly reflects the indispensable role of sensitizer Pr^{3+} in producing the Gd^{3+} persistent luminescence in the $Sr_3Gd_2Si_6O_{18}:Pr^{3+}$ phosphor.

The above design method is general and can be used to fabricate more other Gd^{3+}-activated, Pr^{3+}-sensitized NB-UVB persistent phosphors based on existing Pr^{3+}-activated UVC persistent phosphors. By incorporating certain amount of Gd^{3+} ions into four other types of Pr^{3+}-activated, silicate-based UVC persistent phosphors in ref. 25, represented by the melilite structured $Ca_2Al_2SiO_7:Pr^{3+}$, oxyorthosilicate structured $Lu_2SiO_5:Pr^{3+}$, garnet structured $Ca_3Al_2Si_3O_{12}:Pr^{3+}$ and orthosilicate structured $LiYSiO_4:Pr^{3+}$, we, respectively, obtained NB-UVB persistent phosphors of $Ca_{1.8}Gd_{0.2}Al_2SiO_7:Pr^{3+}$, $Lu_{1.8}Gd_{0.2}SiO_5:Pr^{3+}$, $Ca_{2.8}Gd_{0.2}Al_2Si_3O_{12}:Pr^{3+}$ and $LiY_{0.8}Gd_{0.2}SiO_4:Pr^{3+}$ (Fig. S2, ESI†).

For the Gd^{3+} NB-UVB persistent phosphors developed from Pr^{3+}-activated UVC persistent phosphors, the persistent energy transfer is from the Pr^{3+} 4f5d emitting state to the Gd^{3+} ^6I_J energy levels. Equally important as this energy transfer route, according to Fig. 1, is persistent energy transfer from the Pr^{3+} 4f5d emitting state to the lower energy ^6P_J levels of Gd^{3+}. This, however, requires the Pr^{3+}-activated benchmark phosphor to emit in the UVB region with the Pr^{3+} 4f5d emitting state overlapping with the Gd^{3+} ^6P_J levels. To test this idea, we first developed a Pr^{3+}-activated UVB persistent phosphor $Y_3Al_2Ga_3O_{12}:Pr^{3+}$, and then substituted one-third of its Y^{3+} ions with Gd^{3+} ions, forming a garnet-structured $Y_2GdAl_2Ga_3O_{12}:Pr^{3+}$ phosphor, which has the same structure as the benchmark compound $Y_3Al_2Ga_3O_{12}$ (ICDD 04-007-4274)[27] (Fig. S1b, ESI†). Figure 3a shows the normalized photoluminescence excitation and emission spectra of $Y_3Al_2Ga_3O_{12}:Pr^{3+}$ and $Y_2GdAl_2Ga_3O_{12}:Pr^{3+}$ phosphors. Under excitation at 283 nm, the $Y_3Al_2Ga_3O_{12}:Pr^{3+}$ phosphor exhibits a broadband emission from Pr^{3+} peaking at ~307 nm originating from the Pr^{3+} 4f5d $\rightarrow$ $^3H_{4,5}$ emission transitions (the blue dash line curve). This UVB emission band indicates that the energy of the Pr^{3+} 4f5d emitting state in the $Y_3Al_2Ga_3O_{12}:Pr^{3+}$ phosphor matches that of the Gd^{3+} ^6P_J levels; therefore, energy transfer from the Pr^{3+} 4f5d emitting state to the Gd^{3+} ^6P_J levels is likely to occur in the $Y_2GdAl_2Ga_3O_{12}:Pr^{3+}$ phosphor. Indeed, under excitation at 283 nm, the Pr^{3+} 4f5d $\rightarrow$ $^3H_{4,5}$ emission transition in the $Y_2GdAl_2Ga_3O_{12}:Pr^{3+}$ phosphor gives way to the Gd^{3+} $^6P_{7/2} \rightarrow {}^8S_{7/2}$ emission transition, resulting in strong Gd^{3+} emission at 311 nm (the red solid line curve). The energy transfer from the Pr^{3+} 4f5d emitting state to the Gd^{3+} ^6P_J levels is further verified by the excitation spectra. The excitation spectrum of the $Y_2GdAl_2Ga_3O_{12}:Pr^{3+}$ phosphor monitored at the Gd^{3+} 311 nm emission (the black solid line curve) is identical to that of $Y_3Al_2Ga_3O_{12}:Pr^{3+}$ phosphor monitored at the Pr^{3+} 307 nm emission (the magenta dot-dash line curve); both consist of one strong broad band peaking at 283 nm and one small band peaking at ~244 nm, which correspond to a transition from the $^3H_4$ ground state to the lowest 4f5d state of Pr^{3+} (labeled as $4f5d_1$) and a transition from the $^3H_4$ state to a higher 4f5d state of Pr^{3+} (labeled as

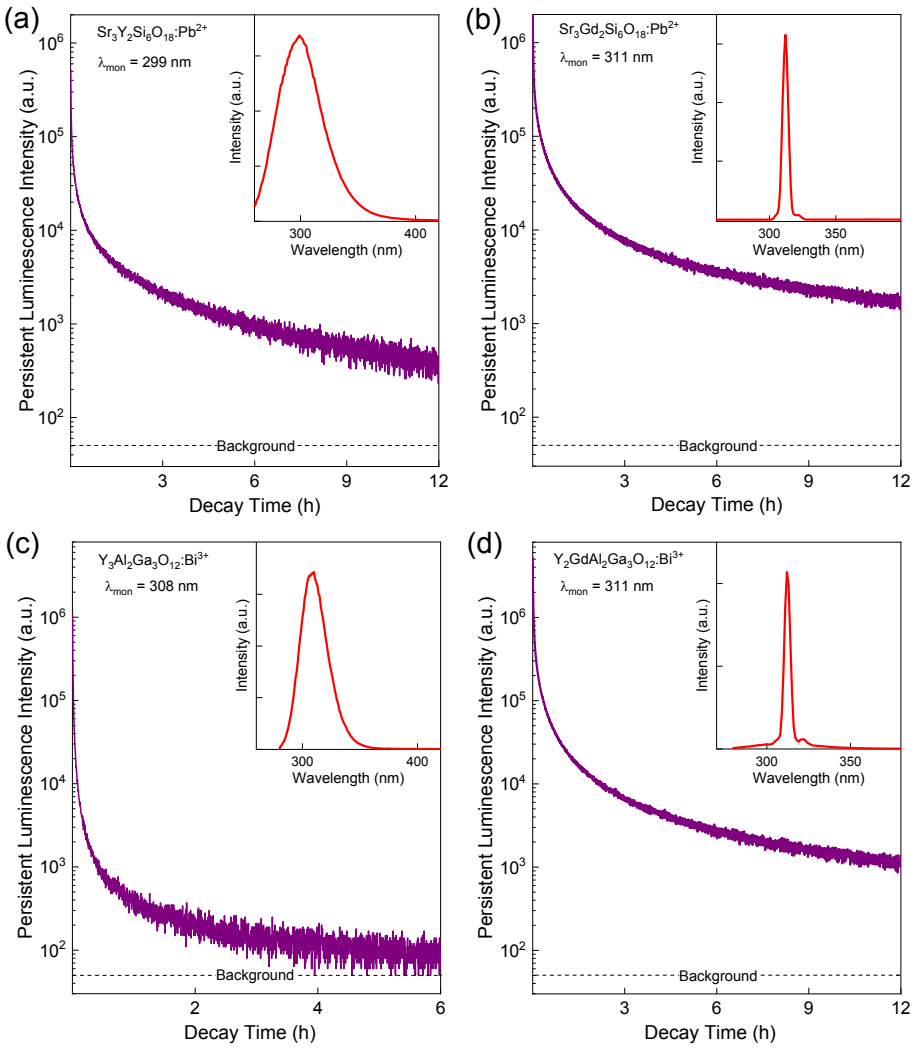

Fig. 4 Persistent luminescence decay curves of Gd^{3+} NB-UVB persistent phosphors developed from Pb^{2+}- and Bi^{3+}-activated UVB persistent phosphors. (a) $Sr_3Y_2Si_6O_{18}:Pb^{2+}$ UVB persistent phosphor. (b) $Sr_3Gd_2Si_6O_{18}:Pb^{2+}$ NB-UVB persistent phosphor. (c) $Y_3Al_2Ga_3O_{12}:Bi^{3+}$ UVB persistent phosphor. (d) $Y_2GdAl_2Ga_3O_{12}:Bi^{3+}$ NB-UVB persistent phosphor. The phosphors were pre-irradiated by a 254 nm lamp for 5 min. The inset in each figure shows the persistent luminescence emission spectrum recorded at 10 min decay.

$4f5d_2$), respectively.[28] After the excitation is ceased, the $Y_3Al_2Ga_3O_{12}:Pr^{3+}$ phosphor exhibits long-lasting Pr^{3+} persistent luminescence in the UVB (at ~307 nm), while for the $Y_2GdAl_2Ga_3O_{12}:Pr^{3+}$ phosphor, as expected, the energy released to the Pr^{3+} 4f5d emitting state from the trapping states is continuously and efficiently transferred to the Gd^{3+} ^6P_J levels, producing Gd^{3+} persistent luminescence in the NB-UVB (Fig. 3b).

In above discussion, we used Pr^{3+}/Gd^{3+} energy transfer ion pair to demonstrate the design of Gd^{3+}-activated, Pr^{3+}-sensitized NB-UVB persistent phosphors. In addition to Pr^{3+}, our design principle is also valid for other sensitizers of Gd^{3+}, provided that these sensitizers activated UVC or UVB persistent phosphors are available. As a test, we developed a Pb^{2+}-activated UVB persistent phosphor $Sr_3Y_2Si_6O_{18}:Pb^{2+}$, which exhibits a broadband persistent luminescence peaking at 299 nm (attributed to the Pb^{2+} $^3P_1 \rightarrow {}^1S_0$ emission transition) for longer than 12 h (Fig. 4a). The $^3P_1$ emitting level of Pb^{2+} in the $Sr_3Y_2Si_6O_{18}:Pb^{2+}$ phosphor overlaps with the ^6P_J levels of Gd^{3+}; therefore, when the Y^{3+} ions in the $Sr_3Y_2Si_6O_{18}:Pb^{2+}$ phosphor are substituted by Gd^{3+} ions, the resulting $Sr_3Gd_2Si_6O_{18}:Pb^{2+}$ material (see crystal structure in Fig. S1a, ESI†) becomes an excellent Gd^{3+} NB-UVB persistent phosphor with an afterglow time of more than 12 h (Fig. 4b). Another material is the Bi^{3+}-sensitized $Y_2GdAl_2Ga_3O_{12}:Bi^{3+}$ NB-UVB persistent phosphor (see crystal structure in Fig. S1b, ESI†) developed from a Bi^{3+}-activated UVB persistent phosphor $Y_3Al_2Ga_3O_{12}:Bi^{3+}$. After charged by a 254 nm lamp, the $Y_3Al_2Ga_3O_{12}:Bi^{3+}$ phosphor emits Bi^{3+} broadband persistent luminescence peaking at ~308 nm (attributed to the Bi^{3+} $^3P_1 \rightarrow {}^1S_0$ emission transition) (Fig. 4c), while the $Y_2GdAl_2Ga_3O_{12}:Bi^{3+}$ phosphor exhibits long-time Gd^{3+} 311 nm persistent luminescence due to the efficient persistent energy transfer from the $^3P_1$ emitting level of Bi^{3+} to the ^6P_J levels of Gd^{3+} (Fig. 4d).

Above we have demonstrated the design and fabrication of eight Gd^{3+} NB-UVB persistent phosphors. It is worth noting that our extensive synthesis work reveals that the Gd^{3+} content in the above-mentioned NB-UVB persistent phosphors can be tuned over a great range. For instance, the general chemical formula of the Gd^{3+}-containing NB-UVB persistent phosphors developed from the $Sr_3Y_2Si_6O_{18}:Pb^{2+}$ UVB persistent phosphor can be written as $Sr_3Y_{2-x}Gd_xSi_6O_{18}:Pb^{2+}$, where x can vary from 0.1 to 2.0 (when x = 2.0, the resulting material is the $Sr_3Gd_2Si_6O_{18}:Pb^{2+}$ phosphor in Fig. 4b), and these Gd^{3+} persistent phosphors exhibit comparable persistent luminescence performance (Fig. S3, ESI†). Moreover, our synthesis work also showed that some ions in some hosts can be substituted by other ions of the same group. For instance, the Y^{3+} ions in the $Y_3Al_2Ga_3O_{12}$ host can be substituted by Lu^{3+} ions to form $Lu_3Al_2Ga_3O_{12}$ host; therefore, more UVB and NB-UVB persistent phosphors can be fabricated such as the UVB persistent phosphors $Lu_3Al_2Ga_3O_{12}:Pr^{3+}$ (Fig. S4a, ESI†) and $Lu_3Al_2Ga_3O_{12}:Bi^{3+}$ (Fig. S5a, ESI†) and the NB-UVB persistent phosphors $Lu_2GdAl_2Ga_3O_{12}:Pr^{3+}$ (Fig. S4b, ESI†) and $Lu_2GdAl_2Ga_3O_{12}:Bi^{3+}$ (Fig. S5b, ESI†). Finally, our design concept is expected to lead to the discovery of more Gd^{3+} NB-UVB persistent phosphors sensitized by not only Pr^{3+}, Pb^{2+} and Bi^{3+}, but also Ce^{3+} (note: we have not identified Ce^{3+}-activated UVC or UVB persistent phosphors; moreover, we have not found the hosts for the Pb^{2+} and Bi^{3+} UVC persistent luminescence).

Conclusions

We have proposed and tested a design concept to develop Gd^{3+}-activated NB-UVB persistent phosphors from the Pr^{3+}-, Pb^{2+}- or Bi^{3+}-activated UVC or UVB persistent phosphors. Guided by this design concept, we have fabricated ten Gd^{3+} NB-UVB persistent phosphors including Pr^{3+}-sensitized $Sr_3Gd_2Si_6O_{18}:Pr^{3+}$, $Ca_{1.8}Gd_{0.2}Al_2SiO_7:Pr^{3+}$, $Lu_{1.8}Gd_{0.2}SiO_5:Pr^{3+}$, $Ca_{2.8}Gd_{0.2}Al_2Si_3O_{12}:Pr^{3+}$, $LiY_{0.8}Gd_{0.2}SiO_4:Pr^{3+}$, $Y_2GdAl_2Ga_3O_{12}:Pr^{3+}$ and $Lu_2GdAl_2Ga_3O_{12}:Pr^{3+}$, Pb^{2+}-sensitized $Sr_3Gd_2Si_6O_{18}:Pb^{2+}$, and Bi^{3+}-sensitized $Y_2GdAl_2Ga_3O_{12}:Bi^{3+}$ and $Lu_2GdAl_2Ga_3O_{12}:Bi^{3+}$. Moreover, we have also developed five first-ever Pr^{3+}-, Pb^{2+}- and Bi^{3+}-activated persistent phosphors emitting in the UVB region including $Y_3Al_2Ga_3O_{12}:Pr^{3+}$, $Lu_3Al_2Ga_3O_{12}:Pr^{3+}$, $Sr_3Y_2Si_6O_{18}:Pb^{2+}$, $Y_3Al_2Ga_3O_{12}:Bi^{3+}$ and $Lu_3Al_2Ga_3O_{12}:Bi^{3+}$. Therefore, this study expands the persistent luminescence research to the NB-UVB as well as the broader UVB spectral regions. The realization of Gd^{3+} NB-UVB persistent luminescence can potentially revolutionize the way the NB-UVB light is used. For instance, the Gd^{3+} NB-UVB persistent phosphors may be used as self-sustained glowing NB-UVB radiation sources for phototherapy, as illustrated by the conceptual NB-UVB Band-Aid phototherapy in Fig. S6 (ESI†).

Author Contributions

Zhengwei Pan: Conceptualization, Methodology, Funding acquisition, Supervision, Writing-Reviewing and Editing. **Peter Kner:** Funding acquisition, Supervision, Writing-Reviewing and Editing. **Xianli Wang:** Investigation, Data Curation, Writing - Original Draft. **Yafei Chen:** Investigation, Data Curation, Writing-Reviewing and Editing.

Conflicts of interest

There are no conflicts to declare.

Acknowledgements

This work is supported by the US National Science Foundation (DMR-1705707) and the College of Petroleum Engineering and Geosciences, King Fahd University of Petroleum & Minerals. We thank McPherson, Inc. (Chelmsford, MA, USA) for helping measure the photoluminescence excitation and emission spectra.

Notes and references

1 H. E. Alderson, *Arch. Dermatol. Syphilol.*, 1923, **8**, 78.
2 J. A. Parrish, H. A. D. White, T. Kingsbury, M. Zahar and T. B. Fitzpatrick, *Arch. Dermatol.*, 1977, **113**, 1529.
3 T. Fischer, *Acta Derm. Venereol.*, 1976, **56**, 473.
4 T. Fischer, *Acta Derm. Venereol.*, 1977, **57**, 345.
5 J. A. Parrish and K. F. Jaenicke, *J. Invest. Dermatol.*, 1981, **76**, 359.
6 H. van Weelden, H. B. De la Faille, E. Young and J. C. van der Leun, *Br. J. Dermatol.*, 1988, **119**, 11.
7 C. Green, J. Ferguson, T. Lakshmipathi and B. E. Johnson, *Br. J. Dermatol.*, 1988, **119**, 691.
8 W. Westerhof and L. Nieuweboer-Krobotova, *Arch. Dermatol.*, 1997, **13**, 1525.
9 I. B. Walters, L. H. Burack, T. R. Coven, P. Gilleaudeau and J. G. Krueger, *J. Am. Acad. Dermatol.*, 1999, **40**, 893.
10 J. M. Kist and A. S. van Voorhees, *Adv. Dermatol.*, 2005, **21**, 235.
11 M. D. Njoo, J. D. Bos and W. Westerhof, *J. Am. Acad. Dermatol.*, 2000, **42**, 245.
12 K. A. Haykal, J. P. DesGroseilliers and J. Cutan. *Med. Surg.*, 2006, **10**, 234.
13 A. J. de Vries and G. Blasse, *Mater. Res. Bull.*, 1986, **21**, 683.
14 A. M. Srivastava, M. T. Sooieraj, S. K. Ruan and E. Banks, *Mater. Res. Bull.*, 1986, **21**, 1455.
15 A. J. de Vries and G. Blasse, *Mater. Res. Bull.*, 1987, **22**, 1141.
16 T. Jüstel, W. Mayr and P. J. Schmidt, U.S. Patent 8173230, 2012.
17 H. S. Kiliaan and G. Blasse, *J. Electrochem. Soc.*, 1989, **136**, 562.
18 M. Leskelä, M. Saakee and G. Blasse, *Mater. Res. Bull.*, 1984, **19**, 151.
19 T. Matsuzawa, Y. Aoki, N. Takeuchi and Y. Murayama, *J. Electrochem. Soc.*, 1996, **143**, 2670.
20 Z. W. Pan, Y. Y. Lu and F. Liu, *Nat. Mater.*, 2012, **11**, 58.
21 Y. Li, M. Gecevicius and J. R. Qiu, *Chem. Soc. Rev.*, 2016, **45**, 2090.
22 D. Jia, R. S. Meltzer and W. M. Yen, *Appl. Phys. Lett.*, 2002, **80**, 1535.
23 N. Y. Yu, F. Liu, X. F. Li and Z. W. Pan, *Appl. Phys. Lett.*, 2009, **95**, 231110.
24 J. Xu and S. Tanabe, *J. Lumin.*, 2019, **205**, 581.
25 X. L. Wang, Y. F. Chen, F. Liu and Z. W. Pan, *Nat. Commun.*, 2020, **11**, 2040.

26 A. P. TyutyunnikIvan, I. Leonidov, L. L. SuratIvan, F. Berger and V. G. Zubkov, *J. Solid State Chem.*, 2013, **197**, 447.
27 C. B. Zheng, P. X. Xiong, M. Y. Peng and H. L. Liu, *J. Mater. Chem. C*, 2020, **8**, 13668.
28 E. Mihóková, V. Babin, K. Bartosiewicz, L. S. Schulman, V. Čuba, M. Kučera and M. Nikl, *Opt. Mater.*, 2015, **40**, 127.